The Importance of Caprock Heating for Geothermal Heat in Place Calculations: An Appalachian Basin Case Study

Jared D. Smith[1], Guðni Axelsson[2], and Erin R. Camp[3]

[1]School of Civil and Environmental Engineering, Cornell University, Ithaca, NY
[2]ÍSOR – Iceland GeoSurvey, Reykjavík, Iceland
[3]Department of Earth and Atmospheric Sciences, Cornell University, Ithaca, NY

Keywords

Sedimentary basin, heat in place, volumetric resource assessment, reservoir modeling, fractures, low temperature, Appalachian Basin

ABSTRACT

The Appalachian Basin was recently assessed for low temperature geothermal resources. Potential permeable zones were identified from existing oil and gas reservoirs, some of which may be repurposed as geothermal reservoirs. A key metric used to evaluate the favorability of repurposing a permeable zone is the thermal energy production potential. Resource assessments that employ volumetric heat in place methods are commonly used to evaluate this metric. In this paper, the importance of including thermal recharge from rocks surrounding the permeable zones is examined. The rocks that supply thermal recharge are referred to as the "skin" of the permeable zone. Volumetric heat in place methods are used to calculate the thermal energy in the permeable zones, and a dynamic resource assessment is used to calculate the heat transferred into the working fluid (water) from the skin after 50 years of production. This deterministic analysis assumes purely conductive heat transfer from the impermeable skin rocks into two horizontal fractures located above and below the permeable zone. Under the assumption of an injection mass flow rate of 30 kg/s that is evenly distributed over the permeable zone, the magnitude of the skin thermal energy relative to the total thermal energy is only important for permeable zones that are less than 10 m thick. For these thin permeable zones, over a 50 year production timeframe the net pay thickness for harvesting thermal energy can be more than double the thermal energy contained within the volume of the permeable thickness.

Introduction

The Appalachian Basin spans an area of about 480,000 km^2 along the western margin of the Appalachian Mountains from northern Alabama, USA to southern Ontario, Canada (Ryder, 1995). The sedimentary rocks contain siliciclastics and carbonates with some shales and evaporites (Roen and Walker, 1996). The sedimentary rocks are as thick as 10 km proximal to the Appalachian Mountains, and are at least 3 km thick in most of the New York-Pennsylvania-West Virginia region of interest (Patchen et al., 2006). Like many sedimentary basins, oil and gas have been resource targets within the Appalachian Basin for over 150 years, which has resulted in a suite of publically available data about the thermal field and rock properties (AASG, 2015). A recent U.S. Department of Energy funded project by Jordan et al. (2015) used this data to examine the risk of developing low temperature, direct-use geothermal energy in the Appalachian Basin. Two of the risk factors evaluated by Jordan et al. (2015) were the thermal resource quality of the basin (Whealton et al., 2015; 2016; Smith et al., 2015; Smith and Horowitz, 2015; Whealton and Stedinger, 2015; Smith, 2015), and the identification of permeable zones from existing oil and gas reservoirs and carbon sequestration analyses (Camp, 2015a; 2015b). The reservoir database from this work (Cornell University, 2015a) also contained data for each reservoir's lithology and fluid flow nature (i.e., porous media, fractured rock, fractured porous media). These results are summarized in Figure 1 as the predicted mean surface heat flow from Cornell University (2015b), and the thickness of permeable zones for potential geothermal reservoirs from Cornell University (2015a). These permeable zones are located at various depths, and more than one permeable zone may exist in any spatial location.

In order to evaluate the viability of repurposing these permeable zones as geothermal reservoirs, the thermal energy production potential of the permeable zones should be understood. This paper presents a deterministic analysis of the volumetric heat in place for the identified permeable zones in Figure 1, and an evaluation of the heat that would be transferred into the permeable zones from surrounding rocks over a production timeframe of 50 years. The heat from surrounding caprock and base rock is referred to as the "skin" of the permeable zone throughout this paper. The skin thermal energy has been shown to be an important thermal recharge source for geothermal reservoirs (e.g. for the Paris Basin, Lopez et al., 2010). Modeling for 50 years is notably longer than the 25 to 30 year timeframe that is commonly used for modeling geothermal reservoirs (O'Sullivan et al., 2000).

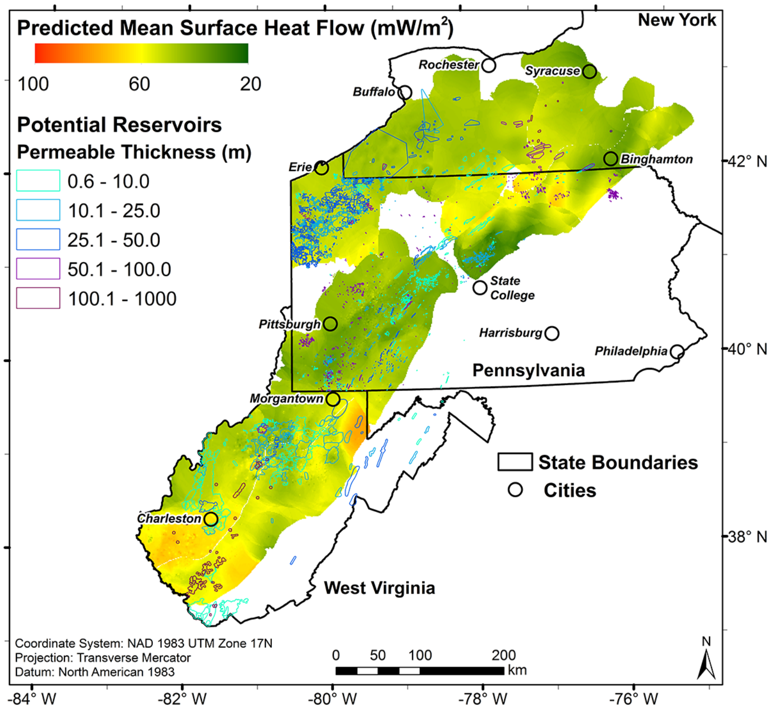

Figure 1. Predicted mean surface heat flow in the Appalachian Basin from Cornell University (2015b), and the thickness of permeable zones in potential reservoirs from Cornell University (2015a). White areas are where no information is available. Cities and state boundaries are shown for reference.

This paper only presents deterministic results because the focus is to demonstrate the importance of skin thickness in volumetric heat in place calculations. The uncertainty in these results should be quantified (e.g. by Monte Carlo analysis in Sarmiento et al., [2013]) but is left to future work.

Methods

The traditional methods for estimating the heat in place include Muffler and Cataldi (1978) and Nathenson (1975), which are adopted and summarized in this paper. To obtain the temperature at depth throughout the thickness of the permeable zones, the one dimensional heat conduction model explained in Smith and Horowitz (2015) was used (code available in Horowitz et al. [2015]). Inputs to this model included the predicted mean surface heat flow at each reservoir location at a spatial resolution of 1 km^2 (Figure 1), and generalized thermal conductivity stratigraphy provided by the Correlation of Stratigraphic Units of North America (COSUNA) project (AAPG, 1985; data available in Cornell University [2015b]). The output from this model is the temperature at depth within the permeable zones at a vertical resolution of 1 m.

Numerical integration of the computed temperatures at depth was used to calculate the total amount of heat contained within the volume of each permeable zone. The heat in place calculation for the i^{th} 1 km^2 surface area (A_i) in each permeable zone is provided in Equation 1:

$$E_i = A_i \sum_{z_{t,i}}^{z_{b,i}} \left(\phi_i \rho_w C_{p,w} + \left[1 - \phi_i \right] \rho_{r,i} C_{p,r,i} \right) \left(\nabla T_i \, Z + T_{z_t,\,i} - T_{ref} \right) \Delta Z, \quad Z = z - z_{t,i}$$

$$\nabla T = \frac{T_Z - T_{Z_t}}{Z} \qquad (1)$$

where E is the thermal energy, ϕ is the porosity of the rock, ρ_w is the density of water, ρ_r is the density of the rock, $C_{p,w}$ is the heat capacity of water, $C_{p,r}$ is the heat capacity of the rock, Z is the depth below the top of the permeable zone z_t, T_{Z_t} is the temperature at the top of the permeable zone, T_Z is the temperature at depth z in the permeable zone, and T_{ref} is the reference temperature, taken as 40 °C. For numerical integration of Equation 1, the thermal gradient, ∇T, is computed between each 1 m depth increment, ΔZ.

The porosity and permeability of the permeable zones were specified on a reservoir-specific basis in Cornell University (2015a). The density and specific heat capacity were not available in this database, so they were gathered from Compare Rocks (2016) according to lithology (Table 1). The thermal conductivity in Table 1 is for water saturated rock, and represents the average for each lithology contained within Smith et al. (2015) calculated for Appalachian Basin formations. No adjustments to these properties were made for temperature and pressure because these effects have not been well studied for the Appalachian Basin, and few of these values are specific to Appalachian Basin rocks. For simplicity, the properties of water were taken at 65 °C, which is a common temperature at 2 km depth where many permeable zones are located. To improve accuracy, all thermal properties should be calculated at their temperature and pressure at depth, and basin-specific values should be used, where possible. However, the use of generalized values does not limit the interpretation of the skin thickness importance for heat transfer; only the accuracy of the results is limited to how well the values in Table 1 represent the Appalachian Basin lithologies.

Table 1. Rock properties used for calculating the heat in place. The thermal diffusivity was calculated from the density, the heat capacity (Compare Rocks, 2016), and the thermal conductivity (Smith et al., 2015).

Lithology	Density (kg/m^3)	Specific Heat Capacity (kJ/[kg-K])	Thermal Conductivity (W/[m-K])	Thermal Diffusivity (m^2/s)
Limestone	2500	0.91	3.5	1.54×10^{-6}
Dolomite	2850	0.92	3.5	1.33×10^{-6}
Sandstone	2500	0.92	3.7	1.61×10^{-6}
Mudstone	2600	0.31	2.4	2.98×10^{-6}
Chert	2700	0.74	2.8	1.40×10^{-6}
Unknown	2500	0.60	2.5	1.67×10^{-6}

The total energy for each permeable zone is the summation of the energy contained within the permeable thickness in each 1 km^2 area, Ai, times a recovery factor, as shown in Equation 2:

$$E_{Res} = R_{Res} \sum_{i=1}^{n} E_i, \quad n = \frac{A_{Res}}{A_i} \tag{2}$$

where E_{Res} is the total energy in the volume of the permeable zone, R_{Res} is the recoverable fraction of energy from the permeable zone, and A_{Res} is the total spatial area of the reservoir. Muffler and Cataldi (1978) highlight the use of a recovery factor as a primary limitation of the volumetric resource assessment methodology. In this work the recovery factor is assumed based on the fluid flow geometry of the permeable zone, as shown in Table 2, but it would be more appropriately estimated by numerical analyses of thermal drawdown over time on a reservoir-specific basis (Muffler and Cataldi, 1978; example in Williams [2007]). Reservoirs in the database with an unknown fluid flow nature were assigned a recovery factor of 27.5, equivalent to that of a fractured porous medium reservoir.

Table 2. Recoverable fractions of heat in the volume of permeable zone rock for different fluid flow geometries (Williams et al., 2008; Nathenson, 1975; Gringarten, 1978).

Reservoir Geometry	Recovery Factor (%)
Porous Medium	35
Fracture Flow	12.5
Fractured Porous Medium	27.5
Unknown	27.5

Volumetric heat in place methods like these do not adequately represent the dynamics of extracting heat from the permeable zone rock over the lifetime of the geothermal system (Axelsson and Dong, 1998). For example, in this work, the recoverable fractions in Table 2 may not correspond to the heat that would be extracted from the permeable zone alone over the 50 year production timeframe that is assumed for calculating thermal recharge from the skin thickness. A more accurate evaluation of the thermal production from the permeable zone may be obtained from numerical modeling of the heat transfer over the production lifetime for these different reservoir geometries. This is beyond the scope of this paper.

Another limitation of the traditional heat in place calculations is the lack of consideration for thermal recharge from the skin rocks (Muffler and Cataldi, 1978). This work considers a worst-case scenario of completely impermeable skin rocks that provide thermal recharge by conduction. These skin rocks are assumed to have infinite thickness and the same geologic properties as the permeable zones because detailed lithologic information about these rocks was not readily available. A simple model is used to evaluate the heat transfer from the skin rocks into two natural horizontal fractures of 2 mm aperture located at the top and bottom of the permeable zone (Figure 2). This is analogous to fracture modeling in enhanced geothermal systems, for which analytical solutions to the heat transfer have been derived in Bodvarsson (1969; 1974) and more recently discussed in Sutter et al. (2011) in terms of thermal drawdown and recovery over time. A schematic of the permeable zone, two natural horizontal fractures, caprocks and base rocks is provided in Figure 2. This conceptual model is comparable to situations in nature in which there is vertical heterogeneity within a single geologic formation.

In Figure 2, the temperature at every position in the cap rock and base rock after 50 years of production is of interest in order to calculate the thermal energy that is recharging the permeable zone. The analytical solution for advection heat transfer in a fracture (Bodvarsson, 1969; 1974) is used to compute this thermal drawdown using the following equations.

In order to compute the advection heat transfer, the effective mass flow rate along the two fractures was calculated using an assumed injection well mass flow rate of 30 kg/s. This flow rate was assumed to be evenly distributed along the permeable zone, such that an effective mass flow rate through the fractures could be calculated for any permeable thickness and fracture aperture using Equation 3:

$$\dot{m}_e = \frac{2b\dot{m}}{ResThick} \quad (3)$$

where $\dot{m}$ is the effective mass flow through fracture of aperture 2b, and ResThick is the total thickness of the permeable zone over which is distributed. The same fracture aperture of 2 mm was used for all permeable zones, regardless of the geometry specified in Table 2. Equation 3 assumes that the well is an open hole only for the thickness of the permeable zone and the fractures.

For each fracture, the heat transfer coefficient, β, was calculated as the ratio of the caprock or base rock conduction heating constants to the fracture advection constants, as shown in Equation 4:

$$\beta = \frac{k_r H}{\dot{m}_e C_{p,w}} \quad (4)$$

where k_r is the thermal conductivity of the rock, H is the thickness into the page (1 km, pixel resolution), and other terms are as defined previously. Note that Equation 4 only considers the heat transfer on one side of the fracture (i.e. the caprock or the base rock side) because the heat from the permeable zone has been accounted for as part of the volumetric heat in place assessment.

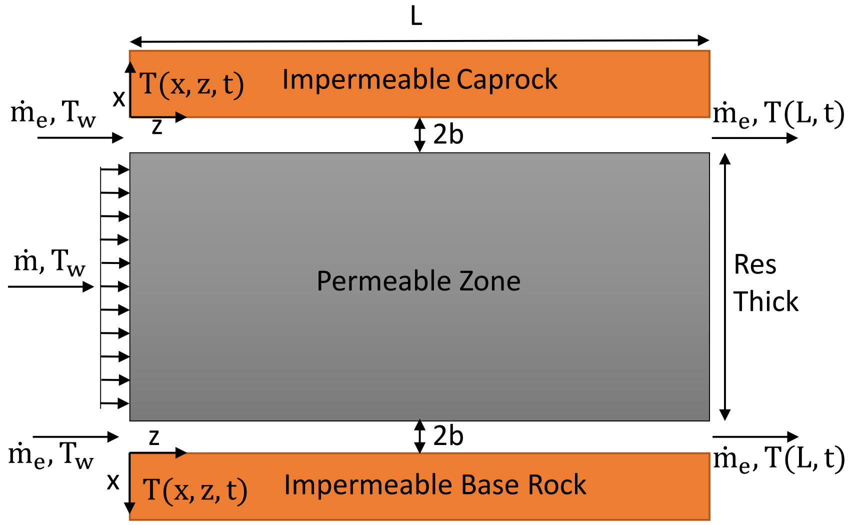

Figure 2. Schematic of the fluid flow and orientation of fractures within a permeable zone that is surrounded by an infinite thickness of impermeable caprock and base rock. An injection well is located on the left, and a production well is located on the right. The fracture half aperture is b, $\dot{m}$ is the mass flow rate of the well, which is evenly distributed along the permeable zone, $\dot{m}_e$ is the effective flow rate through 2b, T_w is the injection water temperature, T(L, t) is the temperature at position L after time t of production, and T(x, z, t) is the temperature within the caprock or base rock at position (x, z) after time t. The caprock and base rock are assumed to have no permeability, but otherwise the same geologic properties as the permeable zone because information about these rocks is not readily available.

To compute the thermal drawdown at all locations in the caprock and base rock, the similarity solution to fracture flow provided in Nathenson (1975) was used, as reproduced in Equation 5:

$$\Theta(x,z,t) \equiv \frac{T(x,z,t) - T_{ref}}{T(x,z,t=0) - T_{ref}} = \mathrm{erf}\left[\frac{x + \beta z}{2\sqrt{\alpha t}}\right] \quad (5)$$

where T(x, z, t) is the temperature in the rock at position (x, z) after time t along the entire extent of the fracture into the page (H, 1 km), α is the thermal diffusivity in Table 1, and other terms have been previously defined. The interest in this equation is the difference between T(x, z, t) and T(x, z, t = 0), which is the temperature drawdown at time t. The temperature drawdown was used in place of $\nabla T_i\, Z + T_{z_t,\, i}$ in Equation 1 to calculate the energy extracted at all locations (x, z) in the caprock and base rock.

A separate calculation was performed for the caprock and the base rock to account for differences in their temperatures at depth, T(x = 0, z = 0, t = 0). These calculations assumed that the entire volume of the caprock and base rock was the same temperature as the temperature at T(x = 0, z = 0, t = 0), and no thermal gradients were considered within the caprock and base rock. Under these assumptions, thermal energy transferred from the base rock will be less, and thermal energy transferred from the caprock will be greater than if thermal gradients were considered.

In order to calculate the thermal drawdown within the caprock and the base rock, the x (vertical) and z (horizontal) dimension were discretized into 1 m increments, and values of the thermal drawdown, T(x, z, t) - T(x, z, t = 0), were computed at each (x, z) coordinate using Equation 5. These coordinates were treated as nodes, and each 1 m^2 cell, composed of the nearest 4 surrounding nodes, was assigned the average of the temperature drawdown in those nodes. The energy extracted in these 1 m^2 cells was calculated using Equation 1 and summed over the x and z dimension in the caprock and base rock to arrive at a skin thermal energy contribution for the permeable zones.

Once the skin thermal energy was calculated, the net pay thickness of the reservoir could be determined. In an active geothermal reservoir, the net pay thickness could be evaluated through means of production history and tracer tests (Williams, 2014), which may implicitly capture the recharge of heat from rocks surrounding the permeable zone. In this work, the net pay thickness is defined as the permeable thickness plus the thickness of rock that would have to be cooled down to the reference temperature such that the skin thermal energy would result, had the skin rocks been a part of the permeable zone and considered in the volumetric heat assessment. The net pay thickness was calculated by the sum of the formation thickness plus this effective skin thickness, as defined in Equation 6:

$$\text{NetPay}_i = \text{ResThick}_i + \frac{E_{skin,\,top,i}}{\left(\phi_i \rho_w C_{p,w} + \left(1-\phi_i\right)\rho_{r,i} C_{p,r,i}\right)\left(T_{z_t,\,i} - T_{ref}\right) A_i} + \frac{E_{skin,\,bot,\,i}}{\left(\phi_i \rho_w C_{p,w} + \left(1-\phi_i\right)\rho_{r,i} C_{p,r,i}\right)\left(T_{z_b,\,i} - T_{ref}\right) A_i} \quad (6)$$

where $E_{skin,top}$ is the energy contributed from the caprock side, and $E_{skin,bot}$ is the energy contributed from the base rock side for the i^{th} 1 km^2 area, A_i. The right two terms are the effective skin thickness portions of Equation 6, which solves Equation 1 for Z in the caprock and base rock.

Some locations in the basin have multiple permeable zones at depth, such that a well could produce in all of the permeable zones simultaneously. Calculations here have treated each permeable zone independently, such that no thermal interaction is considered. Additionally, these calculations assume that an injection and production well doublet is located 1 km apart, and each 1 km^2 area of the reservoir spatial extent has a well doublet. This may be an optimistic scenario of well coverage, even if all reservoirs were fully developed.

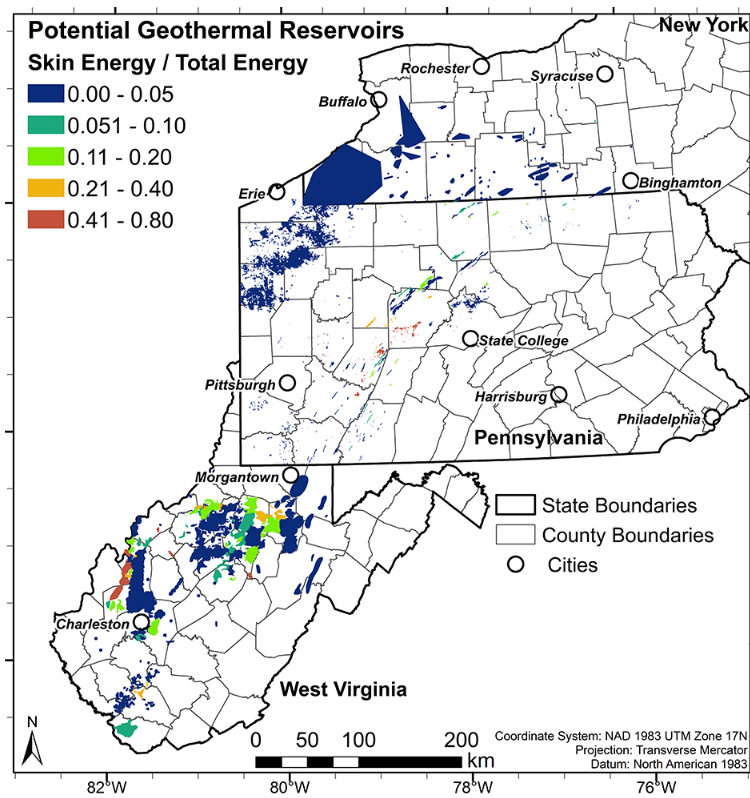

Figure 3. Proportion of the total thermal energy (permeable plus skin) that results from the skin thickness of the reservoir. Larger numbers indicate that relatively more thermal energy is from the skin than from the volumetric thermal energy in the permeable zone.

Results and Discussion

The total thermal energy for each permeable zone is the sum of the volumetric thermal energy plus the skin thermal energy. The ratio of the skin thermal energy to the total thermal energy for each permeable zone is shown in Figure 3. For some reservoirs, the skin thermal energy contributes more than 40% of the total thermal energy over a 50 year production timeframe. However, for the majority of the reservoirs, the skin thermal energy contributes less than 5% of the total thermal energy. It is useful to examine this ratio according to the permeable thickness of the formation, as shown in Figure 4.

Figure 4 shows that the skin thermal energy contribution is important for permeable zones that are less than 10 meters thick, under the assumptions of a mass flow rate of 30 kg/s and fracture aperture of 2 mm. As the permeable thickness decreases from 10 m to 1 m, the percentage of energy that is contributed from the skin increases from less than 10% to as great as 75%, with some differences in the overall trend resulting from lithology (thermal diffusivity) and the temperature in the permeable zones. The spatial locations of these thinner reservoirs stand out in Figure 3 as those reservoirs that are not dark blue.

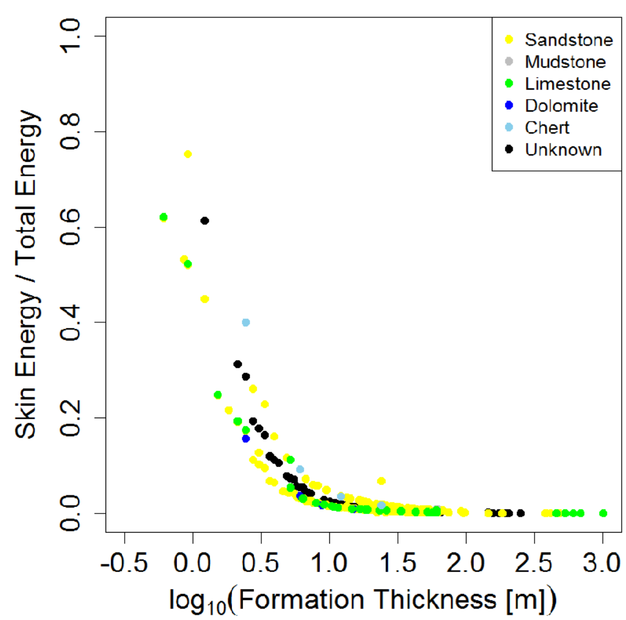

Figure 4. The proportion of the total energy that is contributed from the skin thickness according to the formation thickness and lithology. Results are shown for a mass flow rate of 30 kg/s and a fracture aperture of 2 mm. For reservoirs that are 10 m or thinner, the skin contribution to the total thermal energy is important.

The net pay thickness relative to the permeable thickness is an alternative method for analyzing the heat contribution from the skin thickness, as shown in Figure 5. For most reservoirs the net pay thickness is no more than 5% greater than the permeable thickness, but some reservoirs are effectively more than double the size when the skin thermal energy is considered.

The effective skin thickness is entirely dependent on the thermal properties of the reservoir and the effective mass flow rate through the fractures. In this case, the effective mass flow rate through a fracture of 2 mm aperture is different for each reservoir as a result of different reservoir thickness, as shown in Figure 4. Another useful way to visualize this effect is provided in Figure 6, which relates the effective skin thickness to the effective mass flow rates through the various lithologies, and also compares the effective skin thickness for 2 mm fractures versus 2 cm fractures. An order of magnitude difference in fracture apertures results in an order of magnitude difference in the effective skin thickness and the effective mass flow rate. The effective skin thickness increases fairly linearly with increasing effective mass flow rate, and the more thermally diffuse rock experiences greater effective skin thickness. In both plots it appears that there is a minimum effective skin thickness at low mass flow rates. This may be a result of the discretization used in this analysis, but it should be evaluated further. Fox et al. (2015) evaluate some effects of variable fracture aperture and fracture orientations that are not considered in this work.

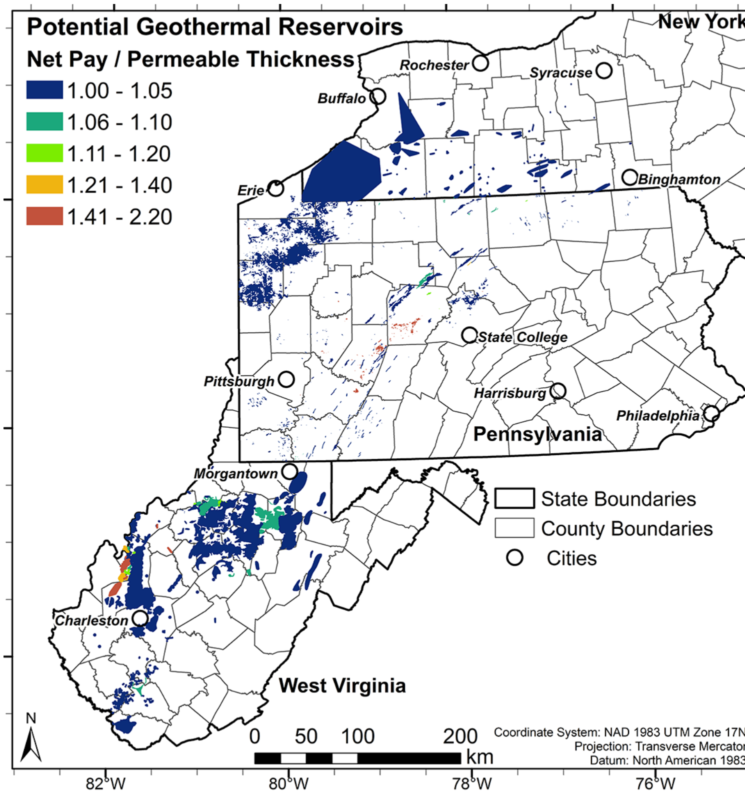

Figure 5. The net pay thickness relative to the permeable thickness. Larger numbers indicate that more energy is contributed from the skin thickness than the volumetric thermal energy in the permeable zone.

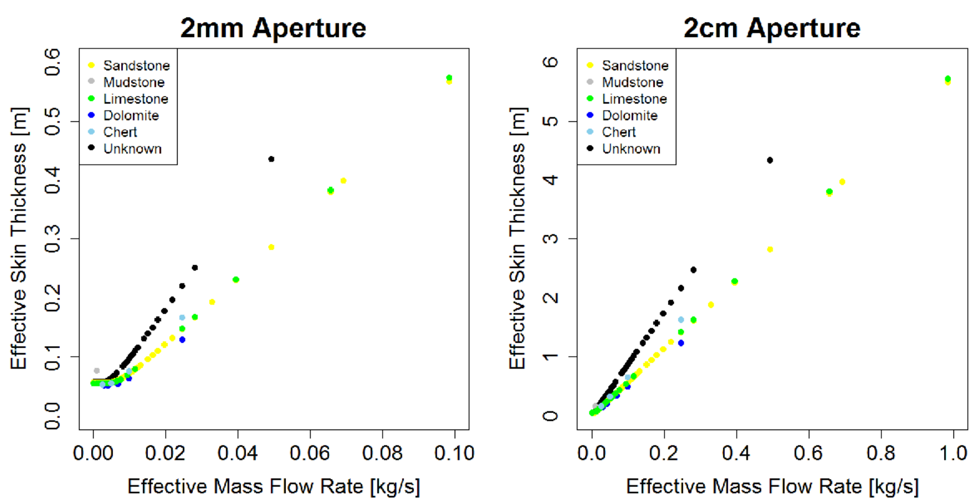

Figure 6. Effective skin thickness of the reservoirs according to their lithology and mass flow rate. Left – 2 mm aperture. Right – 2 cm aperture.

Conclusions

This paper evaluates the importance of including the thermal energy recharge from rocks surrounding permeable zones in calculations of the heat in place for geothermal reservoirs. This "skin thickness" of permeable zones is shown to be an important contribution to the total energy for those permeable zones that are thin, within which the effective mass flow rate is high. For some thin reservoirs, the net pay thickness for thermal energy is more than double the thickness of the permeable zone. Therefore, if thermal recharge from surrounding rocks is not considered, the total energy extracted from these thinner reservoirs may be greatly underestimated. Importantly, this work only addresses a worst-case scenario of conduction heating from impermeable skin rocks, so the thermal energy contribution from the skin may be even greater if they are permeable. Future work should address the geometric complexities of geothermal reservoirs that were not considered here, and evaluate the resulting contribution to the total thermal energy.

References

American Association of Petroleum Geologists (AAPG), 1985. Northern Appalachian region correlation chart. D.G. Patchen, K.L. Avary, and R.B. Erwin, regional coordinators.

American Association of State Geologists (AASG), 2015. Geothermal Data Repository. http://repository.stategeothermaldata.org/repository/browse/.

Axelsson, G., and Z. Dong, 1998. The Tanggu geothermal reservoir (Tianjin, China). *Geothermics, 27(3)*. p. 271-294.

Bodvarsson, G., 1969. On the temperature of water flowing through fractures. *J. Geophys. Res. 74(8)*. p. 1987-1992.

Bodvarsson, G., 1974. Geothermal resource energetics. *Geothermics, 3(3)*. p. 83-92.

Camp, E.R., 2015a. Methodology memo 11: Natural reservoirs task methodology, In *Low Temperature Geothermal Play Fairway Analysis for the Appalachian Basin: Final Phase 1 Research Report*, U.S. Dept. of Energy Award No. DE-EE0006726. Principal Investigator Teresa Jordan. Submitted Oct. 16, 2015.

Camp, E.R., 2015b. Methodology memo 12: Reservoir database inputs, In *Low Temperature Geothermal Play Fairway Analysis for the Appalachian Basin: Final Phase 1 Research Report*, U.S. Dept. of Energy Award No. DE-EE0006726. Principal Investigator Teresa Jordan. Submitted Oct. 16, 2015.

Compare Rocks, 2016. Sedimentary Rocks. Accessed May 5 2016. Available online http://www.comparerocks.com.

Cornell University, 2015a. Appalachian Basin play fairway analysis: Geologic reservoir content model from low-temperature geothermal play fairway analysis for the Appalachian Basin (GPFA-AB) [data set]. Retrieved from http://gdr.openei.org/submissions/561.

Cornell University, 2015b. Thermal quality analysis in low-temperature geothermal play fairway analysis for the Appalachian Basin (GPFA-AB [data set]). Retrieved from http://gdr.openei.org/submissions/638.

Fox, D.B., D.L. Koch, and J.W. Tester, 2015. The effect of spatial aperture variations on the thermal performance of discretely fractured geothermal reservoirs. *Geothermal Energy 3(21)*. 29 p.

Gringarten, A, 1978. Reservoir lifetime and heat recovery factor in geothermal aquifers used for urban heating. *Pure and Applied Geophysics, 117(1, 2)*, p. 295-308.

Horowitz, F.G., J.D. Smith, and C.A. Whealton, 2015. One dimensional conductive geothermal Python code [Data repository]. GeothermalCode. Available online https://bitbucket.org/geothermalcode/onedimensionalgeothermalheatconductionmodel.git.

Jordan, T.E., F.G. Horowitz, J.R. Stedinger, J.W. Tester, E.R. Camp, C.A. Whealton, J.D. Smith, B.J. Anderson, K. Welcker, X. He, M.C. Richards, C. Chickering-Pace, M. Hornbach, Z.S. Frone, C. Ferguson, R. Bolat, M.B. Magnani, 2015. Low temperature geothermal play fairway analysis for the Appalachian Basin: Final phase 1 research report. U.S. Dept. of Energy Award No. DE-EE0006726. Principal Investigator Teresa E. Jordan. Submitted Oct. 16, 2015.

Lopez, S., V. Hamm, M. Le Brun, L. Schaper, F. Boissier, C. Cotiche, and E. Giuglaris, 2010. 40 years of Dogger aquifer management in Ile-de-France, Paris Basin, France. *Geothermics, 39(4)*, p. 339-356.

Muffler, P., and R. Cataldi, 1978. Methods for regional assessment of geothermal resources. *Geothermics, 7(2-4)*, p. 53 – 89.

Nathenson, M., 1975. Physical factors determining the fraction of stored energy recoverable from hydrothermal convection systems and conduction-dominated areas. U.S. Geological Survey, Open File Report 75-525, p. 35.

O'Sullivan, M.J., K. Pruess, and M.J. Lippmann, 2000. Geothermal reservoir simulation: The state-of-practice and emerging trends. Proceedings world geothermal congress 2000, Kyushu-Tohoku, Japan, May 28 – June 10. p. 4065-4070.

Patchen, D.G., J.B. Hickman, D.C. Harris, J.A. Drahovzal, P.D. Lake, L.B. Smith, R. Nyahay, R. Schulze, R.A. Riley, M.T. Baranoski, L.H. Wickstrom, C.D. Laughrey, J. Kostelnik, J.A. Harper, K.L. Avery, J. Bocan, M.E. Hohn, and R. McDowell, 2006. A geologic play book for Trenton-Black River Appalachian Basin exploration. DOE Award Number DE-FC26-03NT41856.

Roen, J.B., and B.J. Walker, 1996. The atlas of major Appalachian gas plays. West Virginia Geological and Economic Survey, Publication V-25.

Ryder, R.T., 1992. Digitized by R.D. Crangle Jr., 2002. Stratigraphic framework of Cambrian and Ordovician rocks in the Central Appalachian Basin from Lake County, Ohio, to Juniata County, Pennsylvania. Miscellaneous Investigations Series Map I-2200.

Ryder, R.T., 1995. Appalachian Basin Province (067), *In* D.L. Gautier, G.L. Dolton, K.I. Takahashi, and K.L. Varnes (eds.). *1995 National assessment of United States oil and gas resources--Results, methodology, and supporting data*. U.S. Geological Survey Digital Data Series DDS-30, Release 2, one CD-ROM, 144 p.

Sarmiento, Z.F., B. Steingrimsson, and G. Axelsson, 2013. Volumetric resource assessment. Presented at "Short course V on conceptual modeling of geothermal systems." UNU-GTP and LaGeo. Santa Tecla, El Salvador. February 24 – March 2.

Smith, J.D. and F.G. Horowitz, 2015. Methodology memo 8: Thermal model methods, In *Low Temperature Geothermal Play Fairway Analysis for the Appalachian Basin: Final Phase 1 Research Report*. U.S. Dept. of Energy Award No. DE-EE0006726. Principal Investigator Teresa Jordan. Submitted Oct. 16, 2015.

Smith, J.D., T.E. Jordan, and Z.S. Frone, 2015. Methodology memo 4: Generalized thermal conductivity stratigraphy, In *Low Temperature Geothermal Play Fairway Analysis for the Appalachian Basin: Final Phase 1 Research Report*. U.S. Dept. of Energy Award No. DE-EE0006726. Principal Investigator Teresa Jordan. Submitted Oct. 16, 2015.

Sutter, D., D.B. Fox, B.J. Anderson, D.L. Koch, P.R. von Rohr, and J.W. Tester, 2011. Sustainable heat farming of geothermal systems: A case study of heat extraction and thermal recovery in a model EGS fractured reservoir. Proceedings, thirty-sixth workshop on geothermal reservoir engineering, Stanford, CA, Jan. 31 – Feb. 2.

Waples, D.W., and J.S. Waples, 2004. A review and evaluation of specific heat capacities of rocks, minerals, and subsurface fluids. Part 1: Minerals and nonporous rocks. *Nat. Res. Res., 13(2)*. p. 97-122.

Whealton, C.A., and J.R. Stedinger, 2015. Methodology memo 6: Outlier identification procedure, In *Low Temperature Geothermal Play Fairway Analysis for the Appalachian Basin: Final Phase 1 Research Report*. U.S. Dept. of Energy Award No. DE-EE0006726. Principal Investigator Teresa Jordan. Submitted Oct. 16, 2015.

Whealton, C.A., J.R. Stedinger, and F.G. Horowitz, 2015. Methodology memo 2: Application of generalized least squares regression in bottom-hole temperature corrections, In *Low Temperature Geothermal Play Fairway Analysis for the Appalachian Basin: Final Phase 1 Research Report*. U.S. Dept. of Energy Award No. DE-EE0006726. Principal Investigator Teresa Jordan. Submitted Oct. 16, 2015.

Whealton, C.A., J.R. Stedinger, and F.G. Horowitz, 2016. Application of generalized least squares regression in bottom-hole temperature corrections. Manuscript submitted for publication.

Williams, C.F., 2007. Updated methods for estimating recovery factors for geothermal resources. Proceedings of the thirty-second workshop on geothermal reservoir engineering, Stanford University, Stanford, CA. January 22-24.

Williams, C.F., M.J. Reed, and R.H. Mariner, 2008. A review of methods applied by the U.S. Geological Survey in the assessment of identified geothermal resources. U.S. Geological Survey Open-File Report 2008-1296, 27 p.